Topology optimization is gaining popularity as a primary tool for engineers in the initial stages of design. Essentially, the design domain is broken down into individual pixels, with the material density of each element or mesh point serving as a design variable. The optimization problem is then tackled through mathematical programming and optimization methods that rely on analytical gradient calculation. In this study, topology optimization using honeycomb tessellation elements is explored. Hexagonal elements have the ability to flexibly connect two adjacent elements. The use of the hexagonal element limits the occurrence of the checkerboard pattern to the finite elements of the quadrilateral standard Lagrangian type. A mathematical model is developed with the objective function being the minimum compliance value of the design domain. The element stiffness matrix is constructed using the strain-displacement matrix and the constitutive matrix, assuming a unit Young's modulus. Additionally, optimal conditions are established using Lagrangian multipliers. Two sensitivity and density filtering filters are employed to increase optimization efficiency, prevent the algorithm from reaching a local optimal state, and speed up convergence. If the suggested filter is employed, the objective function achieves a value of c=173,0293 and convergence is attained after 200 iterations. In contrast, without using the filter, the objective function has a larger value (c=186,7922) and convergence occurs at the 27th iteration. The results are significant for optimizing topology to meet specific boundary condition requirements. This paper proposes a novel approach using a combination of filters to advance topology optimization using hexagonal elements in future applications

Keywords: topology optimization, boundary conditions, isotropic material, filter sensitivity, honeycomb tessell

UDC 629
DOI: 10.15587/1729-4061.2023.277909

TOPOLOGY OPTIMIZATION FOR ISOTROPIC ELASTIC MATERIALS USING HONEYCOMB TESSELL

Ngoc-Tien Tran
Doctor of Mechanical Engineering
Department of Mechatronics Engineering
Hanoi University of Industry
Cau Dien str., 298, Bac Tu Liem District, Hanoi, Vietnam, 100000
E-mail: tientn@haui.edu.vn

Received date 02.02.2023
Accepted date 20.04.2023
Published date 30.04.2023

How to Cite: *Tran, N.-T. (2023). Topology optimization for isotropic elastic materials using honeycomb tessell. Eastern-European Journal of Enterprise Technologies, 2 (7 (122)), 43–49. doi: https://doi.org/10.15587/1729-4061.2023.277909*

1. Introduction

Topology optimization (TO) is a technique used in engineering design to achieve optimized designs while reducing costs. It involves determining the most efficient material distribution in a given design space to satisfy given boundary conditions [1–3]. TO is applied in structural design, fluid flow optimization, material design and additive manufacturing [4–6]. In recent years, TO has been studied by many scientists. In [7], the authors employed a parameterized cellular model and a multiscale TO approach to predict bone remodeling around an uncemented femoral implant. In [8], the authors explored the application of a virtual phase method (VPM) that utilizes structured meshes to effectively address optimization problems featuring intricate geometries and arbitrary non-design components. In [9], the authors introduced a TO approach that combines subtractive and additive manufacturing methods and focuses on remanufacturing. It proposed a design-for-remanufacturing strategy and offers solutions for product upgrades and repairs. The authors in [10] proposed a TO approach that employs finite element analysis of the assembly to achieve reduced weight and mitigate stress analysis distortion. The authors in [11] proposed a TO approach for rarefied gas flow problems, with the objective of determining the optimal structure of a flow channel as a configuration of both gas and solid domains. The authors in [12] introduced a novel method for translating TO outcomes into stereolithography (STL) and parametric computer-aided design (CAD) models. In [13], the authors suggested an evolutionary TO approach for minimizing stress in design, utilizing the bi-directional evolutionary structural optimization (BESO) method. To allow for the TO of geometrically nonlinear structures undergoing significant deformations, the Iso-XFEM technique is expanded through the implementation of a total Lagrangian finite element formulation [14]. The authors in [15] proposed a novel TO approach utilizing the extended finite element method (XFEM) to improve the fracture strength of specific locations in a structure. Therefore, studies that are devoted to the field of TO are scientific relevance.

2. Literature review and problem statement

TO has become a reliable tool for achieving optimized designs in structural, mechanical, and material systems. Despite the maturity of the field, a numerical problem known as the checkerboard problem remains a topic of extensive research. In [16], the authors proposed a node-based implementation in continuum TO that is resistant to element-wise checker boarding instabilities, which can be problematic with element-based design variables. In [17], polygonal meshes constructed using Voronoi tessellations exhibit a higher degree of geometric isotropy and are more flexible in discretizing complex domains, without being influenced by numerical instabilities. In [18], to address checkerboard patterns in topologies, the ground element filtering (GEF) technique is used. Moreover, several authors have investigated filters to reduce the checkerboard phenomenon and enhance the optimization process's performance. The authors in [19] proposed an alternative to the padding method for PDE filtering by using the potential form of the PDE filter. This approach allows the inclusion of penalty terms with a clearly defined physical interpretation. Recent studies on TO have not yet

implemented a structural optimization approach that utilizes honeycomb hexagonal finite elements with double filters. By utilizing a tessellated honeycomb form, superior connection geometry can be achieved, thereby eliminating the checkerboard patterns and single-point connections that are characteristic of optimized designs [20, 21]. Furthermore, as discussed in [22], the hexagonal finite element structure provides greater numerical accuracy and is well-suited for modeling polycrystalline materials. A new shadow density filter has been created and applied to structural TO with consideration given to molding manufacturability [23]. The authors in [24] introduced a novel density filter technique for TO of coated structures. Unlike previous approaches, this new method solely employs the density filter and its projection, without dependence on the density field's gradient. All this allows to assert that it is expedient to conduct a study on TO for isotropic elastic materials using honeycomb tessell.

3. The aim and objectives of the study

The aim of the study is to perform topology optimization on isotropic elastic materials. This will make it possible to increase performance and completely overcome the checkerboard phenomenon.

To achieve this aim, the following objectives are accomplished:

– to solve the optimization problem, this study designs a domain grid with hexagonal elements and honeycomb structure grids with elements with two degrees of freedom;

– to increase the optimal performance to 11 %, the study conducted optimization using a combination of two filters: sensitivity filtering and density filtering, then compared it with the case where no filters were used.

4. Materials and methods

By implementing this optimization, the mathematical modeling procedure is made more straightforward, implementing the need for element updates, as highlighted in previous research studies [16–19]. With this foundation, the article proposes optimal conditions for implementation based on iterative processes. Furthermore, two filters are developed and combined to improve the optimization process's efficiency and ensure the convergence condition is met.

The optimization problem is assumed to be within a design domain $\Omega\subset\mathbb{R}^2$. The domain is a Lipschitz bounded and open domain simultaneously subject to applied loads and boundary conditions. The boundary $\partial\Omega$ of Ω consists of two disjoint parts $\partial\Omega_u$ and $\partial\Omega_p$. The part $\partial\Omega_u$ consists of zero displacements and $\partial\Omega_p$ is where the applied loads ($\Omega=\partial\Omega_u\cup\partial\Omega_p$ and $\partial\Omega_u\cap\partial\Omega_p=\varnothing$). According to [1], the compliance optimization problem involves minimizing the compliance c within a design domain:

$$\begin{aligned}&\min_{\rho}: \quad c(\rho)=U^TKU=\sum_{e\in N_e}u_e^Tk_eu_e=\sum_{e\in N_e}E_e(\rho_e)u_e^Tk_0u_e\\&s.t.: \quad V(\rho)=\sum_{e\in N_e}\rho_ev_e=\varsigma V_0;\ \ 0\le\varsigma\le1\\&\qquad KU=F\\&\qquad 0\le\rho_{\min}\le\rho_e\le1;\ \ \forall e\in N_e,\end{aligned}\tag{1}$$

where F is the vector of nodal forces; U is the global displacement; K is global stiffness matrix; u_e and k_0 are the element displacement vector and stiffness matrix, respectively; ρ is the vector of design variables; $\rho_{\min}$ is non-zero to avoid singularity; ρ_e is the value representing the elemental material density $e\in N_e$ (when $\rho_e=0$, the material is considered to be in a hollow state, while $\rho_e=1$ indicates that the material is in a solid state). N_e is a set of finite element indices; the finite element assembly operator is denoted as $\sum$; while V, v_e and V_0 represent the material volume, the volume of material in element e, and design domain volume, respectively; the prescribed volume fraction is represented by the variable ζ. To enhance the convergence speed of the optimization problem, the modified SIMP approach is utilized along with a power-law interpolation penalty formulation [1]. In this method, the element Young's modulus E_e is expressed as a power function of the design variable:

$$E_e(\rho_e)=E_{\min}+(E_0-E_{\min})\rho_e^p,\tag{2}$$

where $E_{\min}$ is an extremely small value to avoid singularities in the stiffness matrix, p is the is a penalization factor (typically p=3). E_0 is the stiffness of the material. The element stiffness matrix is given by:

$$k_e(\rho_e)=E_e(\rho_e)k_0=E_e(\rho_e)\int_{v_e}B_0^TD_0B_0\mathrm{d}v_e,\tag{3}$$

where B_0, D_0 are the strain–displacement matrix and the constitutive matrix with unit Young's modulus, respectively. Let ϑ be the Poisson's ratio of the isotropic material, the constitutive matrix is given by:

$$D_0=\frac{1}{(1+\vartheta)(1-2\vartheta)}\times\begin{bmatrix}1-\vartheta&\vartheta&\vartheta&0&0&0\\\vartheta&1-\vartheta&\vartheta&0&0&0\\\vartheta&\vartheta&1-\vartheta&0&0&0\\0&0&0&(1-2\vartheta)/2&0&0\\0&0&0&0&(1-2\vartheta)/2&0\\0&0&0&0&0&(1-2\vartheta)/2\end{bmatrix}.\tag{4}$$

The process of discretizing the design domain involves dividing it into adjacent hexagons that do not overlap. Within a $\xi(O_1x_1y_1)$ frame, each hexagonal element is defined by its vertices and the circumscribing circle with a radius of 1 unit, represented by $C_v(O_1; r_{v=}1)$ (Fig. 1). From Fig. 1, the coordinates of the hexagonal vertices can be obtained:

$$\left(V_x^i;V_y^i\right)\equiv\left(\cos\frac{(2i-1)\pi}{6};\sin\frac{(2i-1)\pi}{6}\right).\tag{5}$$

NeX and NeY represent the count of hexagonal elements in the x and y directions, respectively. Each element is composed of six nodes, and each node has two degrees of freedom (DOFs). In the $\xi_f(O_fx_fy_f)$ frame (Fig. 2), the vertex coordinates of a honeycomb cell are expressed:

$$\begin{cases}\left(V_x^{\varepsilon};V_{y-k}^{\sigma}\right)\equiv\left(\varepsilon a\cos\left(\frac{\pi}{6}\right);a\left(1.5\sigma+\frac{(-1)^k}{2}\sin\left(\frac{\pi}{6}\right)\right)\right),\\k=1,2,\\\varepsilon=0,1,2,...,2NeX;\sigma=0,1,2,...,NeY,\end{cases}\tag{6}$$

where a is the edge length of the hexagon.

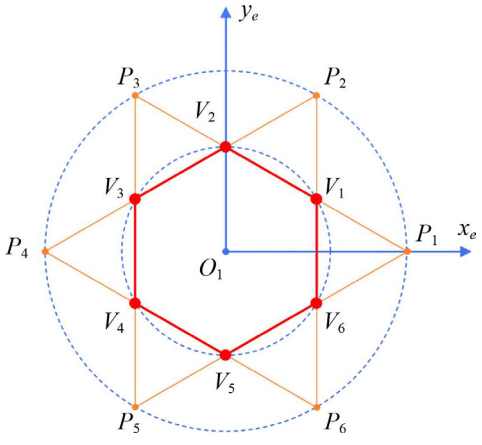

Fig. 1. Hexagonal element

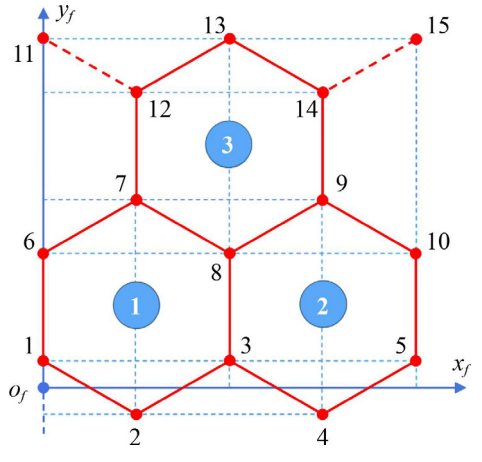

Fig. 2. Grid of hexagonal elements

The standard optimality criteria method (OC) is employed to address the optimization problem stated in (1) [1]. The Lagrangian function associated with the problem is provided:

$$\hat{L}\left(\rho_e,\lambda_e,\lambda_g,\mu_{\rho-},\mu_{\rho+}\right)=U^TKU+\lambda_e\left(\sum_{e\in\mathbb{N}_e}\rho_e v_e-\varsigma V_0\right)+$$
$$+\lambda_g^T\left(KU-F\right)+\sum_{e\in N_e}\mu_{\rho-}\left(-\rho_e+\rho_{\min}\right)+\sum_{e\in N_e}\mu_{\rho+}\left(\rho_e-1\right), \quad (7)$$

where λ_e, λ_g, $\mu_{\rho-}$, $\mu_{\rho+}$ are the Lagrangian multipliers for the constraints of the optimization problem. The optimal state is attained when the conditions relating to the displacement vector and the design variables are met. Therefore, the optimality conditions for the design variables are obtained from (7) and are as follows:

$$\begin{cases}\partial\hat{L}\left(\rho_e,\lambda_e,\lambda_g,\mu_{\rho-},\mu_{\rho+}\right)/\partial U=0,\\ \partial\hat{L}\left(\rho_e,\lambda_e,\lambda_g,\mu_{\rho-},\mu_{\rho+}\right)/\partial\rho_e=0,\\ \partial k_e/\partial\rho_e=p\rho_e^{p-1}\left(E_0-E_{\min}\right)k_0,\end{cases} \quad (8)$$

and switching conditions:

$$\begin{cases}\mu_{\rho-}\geq 0;\mu_{\rho+}\geq 0,\\ \mu_{\rho-}\left(-\rho_e+\rho_{\min}\right)=0,\\ \mu_{\rho+}\left(\rho_e-1\right)=0.\end{cases} \quad (9)$$

Expanding and simplifying (8) results in:

$$p\rho_e^{p-1}\left(E_0-E_{\min}\right)u_e^Tk_0u_e=\lambda_e+\mu_{\rho-}+\mu_{\rho+}. \quad (10)$$

Let $\psi_e:=\lambda_e^{-1}p\rho_e^{p-1}\left(E_0-E_{\min}\right)u_e^Tk_0u_e$ and assumption that each element has unit volume ($\partial V/\partial\rho_e$=1). Thus, in the case of $\rho_e\in(\rho_{\min};1)$ then ψ_e=1 and:

$$\lambda_e=\frac{-\partial c(\rho)}{\partial\rho_e}=p\rho_e^{p-1}\left(E_0-E_{\min}\right)u_e^Tk_0u_e. \quad (11)$$

According to [1], the formula below is utilized to update the design variables:

$$\rho_{e,k+1}=$$
$$=\begin{cases}\max\left(0,\rho_{e,k}-\upsilon\right) & \text{if } \rho_{e,k}\psi_{e,k}^{\eta}\leq\max\left(0,\rho_{e,k}-\upsilon\right),\\ \min\left(1,\rho_{e,k}+\upsilon\right) & \text{if } \rho_{e,k}\psi_{e,k}^{\eta}\geq\min\left(1,\rho_{e,k}+\upsilon\right),\\ \rho_{e,k}\psi_{e,k}^{\eta} & \text{otherwise,}\end{cases} \quad (12)$$

where $\rho_{e,k+1}$ denotes the value of the design variable at iteration k, υ is the move limit, η is the tuning parameter. These values can be adjusted to enhance the convergence and stability of the iterative model, as presented in (12). The new design variable values are dependent on the Lagrangian multiplier. As the iterative process proceeds, the volume of the structure decreases, and the elements that contain the material are gradually eliminated until the optimal state of the compliance value.

The density value of an element is used to indicate the amount of material present at that element. If the element density values in TO problems alternate in a checkerboard pattern with alternating solid and hollow regions, it suggests that the material distribution is suboptimal. In order to eliminate these checkerboard patterns, filtering techniques are employed. The research being conducted utilizes two filtering techniques – sensitivity filtering and density filtering.

In order to prevent the creation of checkerboard patterns during linear elastic texture optimization, the sensitivity filter function is provided as follows:

$$\frac{\partial\hat{c}}{\partial\rho_e}=\frac{1}{\rho_e\sum_{f\in\mathrm{N}_f}\hat{H}_{e,f}}\sum_{f\in\mathrm{N}_f}\rho_f\hat{H}_{e,f}\frac{\partial c}{\partial\rho_f}, \quad (13)$$

where N_f is a set of elements f that are restricted within the circle of the filter mesh with a radius of R (Fig. 3). The convolution operator $\hat{H}_{e,f}$ is defined as follows:

$$\hat{H}_{e,f}=R-\mathrm{dist}\left(e,f\right),$$
$$\left\{e\in\mathrm{N}_e\,|\,dist\left(e,f\right)\leq R\right\},\quad e=1,\ldots,\mathrm{N}_e, \quad (14)$$

where the operator dist(e, f) is the distance between the center element f and the center of element e.

Similar to sensitivity filtering, the density grid in sensitivity filtering comprises elements e as illustrated in (13). The original design variables lack physical significance. However, during the filtering procedure, the design variable elements are substituted by the design variable elements via the density grids. The filtered design variables, which represent the physical density of the elements, are expressed as follows:

$$\tilde{\rho}_e=\frac{\sum_{f\in\mathrm{N}_f}\hat{H}_{e,f}\rho_f}{\sum_{f\in\mathrm{N}_f}\hat{H}_{e,f}}. \quad (15)$$

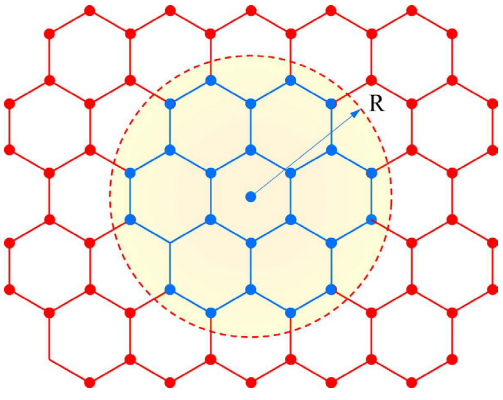

Fig. 3. Filter mesh with a radius

When using density filtering, the material volume and complimance function with respect to the physic density:

$$\frac{\partial \tilde{V}}{\partial \rho_g}=\sum_{e\in N_e}\frac{\partial \tilde{V}}{\partial \tilde{\rho}_e}\frac{\partial \tilde{\rho}_e}{\partial \rho_g}=\sum_{e\in N_e}\frac{1}{\sum_{f\in N_f}\hat{H}_{e,f}}\hat{H}_{f,e}\frac{\partial \tilde{V}}{\partial \tilde{\rho}_e}, \quad (16)$$

$$\frac{\partial \tilde{c}}{\partial \rho_g}=\sum_{e\in N_e}\frac{\partial \tilde{c}}{\partial \tilde{\rho}_e}\frac{\partial \tilde{\rho}_e}{\partial \rho_g}=\sum_{e\in N_e}\frac{1}{\sum_{f\in N_f}\hat{H}_{e,f}}\hat{H}_{g,e}\frac{\partial \tilde{c}}{\partial \tilde{\rho}_e}, \quad (17)$$

where

$$\frac{\partial \tilde{\rho}_e}{\partial \rho_g}=\frac{\hat{H}_{e,g}}{\sum_{f\in N_f}\hat{H}_{e,f}}, \quad (18)$$

(16), (17) show the change in volume and conformance, which characterizes a combined filter of sensivity filtering and density filtering.

5. Research results of topology optimization using honeycomb tessell

5. 1. Hexagonal element grid

The MBB beam's straightforward geometry and flexibility in changing boundary conditions make it a commonly used element in TO. This section examines several numerical examples of MBB beams to demonstrate the effectiveness of a novel methodology. The MBB beam under consideration has the specific shape and boundary conditions illustrated in Fig. 4.

To depict the discrete portion of the design domain (as shown in Fig. 5), the MBB beam is divided into 30×20 and 35×27 hexagonal elements. The cases of NeX and NeY comprise even and odd numbers, respectively.

When NeY is an even number, it results in the elimination of hanging nodes and an update of node numbering.

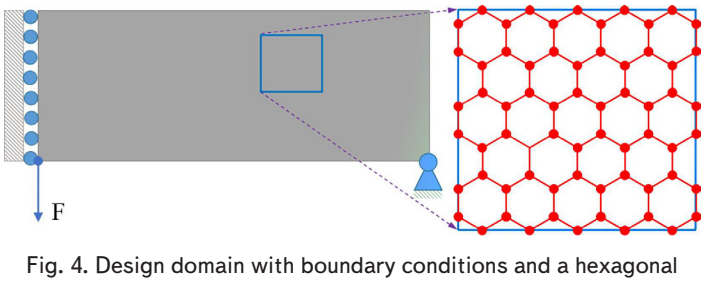

Fig. 4. Design domain with boundary conditions and a hexagonal element grid

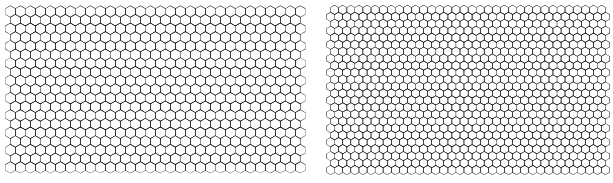

Fig. 5. Design a domain grid with a hexagonal element: *a* – 30×20 hexagonal elements; *b* – 30×20 hexagonal elements

5. 2. Optimization results for scenarios with and without a filter

The penalization factor for the following examples is set to p=3, and the Poisson ratio is ϑ=1/3. The calculations were conducted using a machine with a 64-bit operating system, 16.0 GB RAM, and an Intel(R) Core(TM) i7-8565U CPU 2.9 GHz. The mesh size is 160×65, the volume ratio is ζ=0.5, and the filter radius is $R=1.5\sqrt{3}$. Two scenarios were considered for the optimized results of the design domain depicted in Fig. 6: one without filtering (Fig. 6, *a*–*c*) and another with filters (Fig. 6, *d*, *e*, 7). Please note that in Fig. 6, the yellow area within the rectangular design domain represents the material that was not used in the final design, while the dark purple color represents the optimized structure.

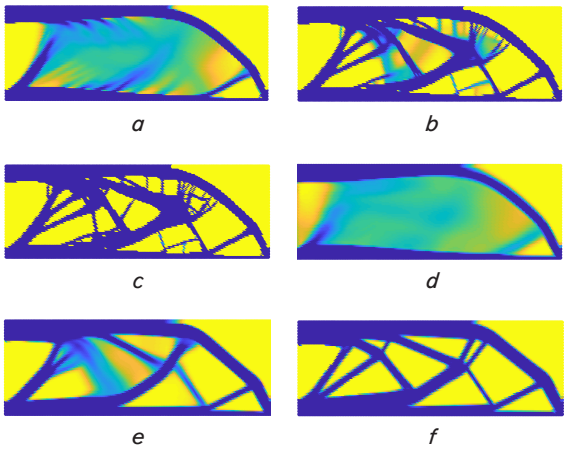

Fig. 6. The optimization results for scenarios with and without a filter; *a* – *c*=229.1963; *b* – *c*=192.1905; *c* – *c*=186.7922; *d* – *c*=253.5322; *e* – *c*=192.3891; *f* – *c*=173.0293

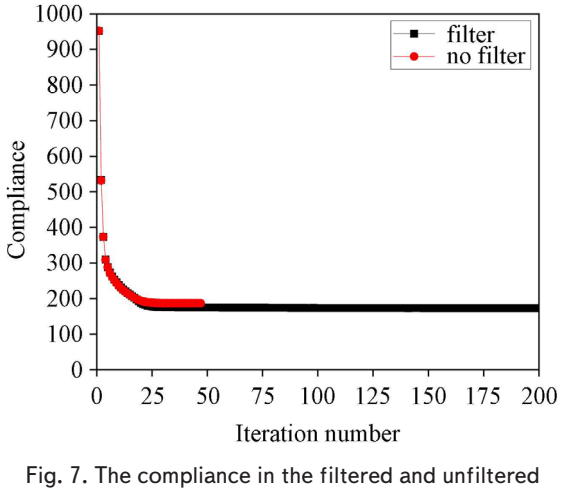

Fig. 7. The compliance in the filtered and unfiltered scenarios

According to the boundary conditions described in Fig. 8, the study to determine the optimal texture with the proposed filter has been presented in Section 4 of the paper. The volume ratio is fixed at ζ=0.4, and the mesh sizes used are 60×60, 120×120, and 180×180.

For each mesh size, the filter radius is set to 0.03 times the length of the design domain, resulting in values of $R=1.8\sqrt{3}$, $R=3.6\sqrt{3}$, $R=5.4\sqrt{3}$, respectively.

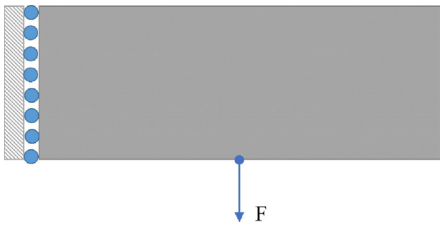

Fig. 8. Design domain with variable grid size

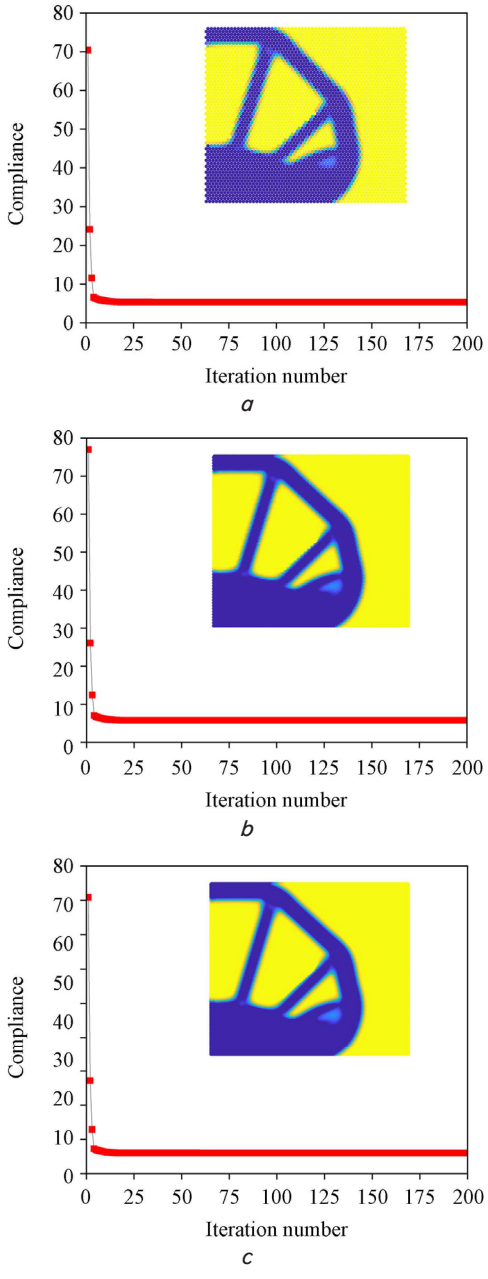

Fig. 9. Optimum structure according to mesh size and filter radius: *a* – 60×60; *b* – 120×120; *c* – 180×180

6. Discussion of results of the study of topology optimization using honeycomb tessell

Fig. 6 illustrates that the optimization method achieves good optimal performance in both scenarios, with and without a filter, without any checkerboard patterns. This is due to the honeycomb tessellation's geometric structure, which automatically breaks any checkerboard patterns as it features edge-to-edge connections between hexagons. This demonstrates the advantage of using honeycomb tessellation in the optimization method presented in the paper. This problem has addressed the challenges faced in previous studies that utilized quadrilateral elements [1, 3, 4]. However, without using a filter, the optimal structures are dependent on the mesh, which can result in uneven edges appearing at the boundary layers of the optimal profile, and numerous small lines that can make fabrication challenging. On the other hand, using the suggested filter yields optimal textures that are independent of the mesh, and thus have the same topology, regardless of the mesh size employed. The utilization of both sensitivity filter and density filter (Fig. 6, *e*–*f*) demonstrated higher efficacy in comparison to having no filter at all (Fig. 6, *a*–*c*). The optimal texture also has a clear structure and lacks the fragmentation that occurs when no filter is used. Furthermore, Fig. 7 shows that when the proposed filter is used, the objective function value is *c*=173.0293, and convergence is achieved at iteration number 200. In contrast, when no filter is used, *c*=186.7922, and convergence occurs at iteration number 27. This indicates that using the filter results in higher optimal performance and a better optimal value compared to not using the filter.

Fig. 9 reveals that the optimal value converges in all three-grid cases by iteration number 175. However, the 60×60 grid case shows the minimum compliance value of *c*=5.3392, followed by the 120×120 grid case with *c*=5.7622, and the largest compliance value of *c*=6.0148 for the 180×180 case. Thus, changing the size of the design grid does not significantly affect the objective function value. Notably, the optimal design domain profile with the 180×180 grid size exhibits less aliasing than the other two cases, indicating that higher resolution leads to reduced aliasing and improved design accuracy. Based on the results, the study's range is constrained to two-dimensional isotropic elastomers. In this study, the boundary of the design domain is approximated by the honeycomb coverage. Hence, the current disadvantage of the study is its reliance on a specific finite element formulation, which necessitates the use of honeycomb finite elements. Additionally, implementing the suggested approach of combining filters necessitates the creation of new material models and 3-dimensional design domains to enable a thorough assessment of the mathematical model's efficacy. In order to be practical, two requirements must be fulfilled:

1) utilization of a mesh that eliminates contact with points and edges;

(2) choosing an appropriate interpolation method for finite elements.

From there, it shows a very potential research direction, which is the optimization of the boundary and filter radius of the filter. Besides, the optimization of the topology using the honeycomb structure and the improved filter of this study promise to be applied to the design of microelectromechanical systems and piezoelectric actuators in the future.

7. Conclusions

1. The study shows that the use of hexagonal elements eliminates checkerboard formation while providing a robust and stable means of solving TO problems.

2. Without using a filter, the optimal structures are dependent on the mesh, which can result in fabrication challenges. The suggested filter this issue and yields optimal textures that are independent of the mesh employed size (the filter radius is set to 0.03 times the length of the design domain). Besides, using the filter results in higher performance and a better optimal value compared to not using the filter. Furthermore, changing the size of the design grid does not significantly affect the objective function value. However, higher resolution leads to reduced aliasing and improved design accuracy.

Conflict of interest

The authors declare that they have no conflicts of interest in relation to the current study, including financial, personal, authorship, or any other, that could affect the study and the results reported in this paper.

Funding

The study was conducted without financial support.

Data availability

All data are available in the main text of the manuscript.

References

1. Sigmund, O. (2007). Morphology-based black and white filters for topology optimization. Structural and Multidisciplinary Optimization, 33 (4-5), 401–424. doi: https://doi.org/10.1007/s00158-006-0087-x
2. Banh, T. T., Luu, N. G., Lee, D. (2021). A non-homogeneous multi-material topology optimization approach for functionally graded structures with cracks. Composite Structures, 273, 114230. doi: https://doi.org/10.1016/j.compstruct.2021.114230
3. Huang, X., Li, W. (2022). Three-field floating projection topology optimization of continuum structures. Computer Methods in Applied Mechanics and Engineering, 399, 115444. doi: https://doi.org/10.1016/j.cma.2022.115444
4. Zhou, P., Du, J., Lü, Z. (2018). A generalized DCT compression based density method for topology optimization of 2D and 3D continua. Computer Methods in Applied Mechanics and Engineering, 334, 1–21. doi: https://doi.org/10.1016/j.cma.2018.01.051
5. Shen, W., Ohsaki, M. (2020). Geometry and topology optimization of plane frames for compliance minimization using force density method for geometry model. Engineering with Computers. doi: https://doi.org/10.1007/s00366-019-00923-w
6. Tarek, M., Ray, T. (2020). Adaptive continuation solid isotropic material with penalization for volume constrained compliance minimization. Computer Methods in Applied Mechanics and Engineering, 363, 112880. doi: https://doi.org/10.1016/j.cma.2020.112880
7. Mathai, B., Dhara, S., Gupta, S. (2022). Bone remodelling in implanted proximal femur using topology optimization and parameterized cellular model. Journal of the Mechanical Behavior of Biomedical Materials, 125, 104903. doi: https://doi.org/10.1016/j.jmbbm.2021.104903
8. Li, H., Li, H., Gao, L., Li, J., Li, P., Yang, Y. (2021). Topology optimization of arbitrary-shape multi-phase structure with structured meshes based on a virtual phase method. Computer Methods in Applied Mechanics and Engineering, 387, 114138. doi: https://doi.org/10.1016/j.cma.2021.114138
9. Liu, J., Zheng, Y., Ma, Y., Qureshi, A., Ahmad, R. (2019). A Topology Optimization Method for Hybrid Subtractive–Additive Remanufacturing. International Journal of Precision Engineering and Manufacturing-Green Technology, 7 (5), 939–953. doi: https://doi.org/10.1007/s40684-019-00075-8
10. Sha, L., Lin, A., Zhao, X., Kuang, S. (2020). A topology optimization method of robot lightweight design based on the finite element model of assembly and its applications. Science Progress, 103 (3), 003685042093648. doi: https://doi.org/10.1177/0036850420936482
11. Sato, A., Yamada, T., Izui, K., Nishiwaki, S., Takata, S. (2019). A topology optimization method in rarefied gas flow problems using the Boltzmann equation. Journal of Computational Physics, 395, 60–84. doi: https://doi.org/10.1016/j.jcp.2019.06.022
12. Liu, S., Li, Q., Liu, J., Chen, W., Zhang, Y. (2018). A Realization Method for Transforming a Topology Optimization Design into Additive Manufacturing Structures. Engineering, 4 (2), 277–285. doi: https://doi.org/10.1016/j.eng.2017.09.002
13. Xia, L., Zhang, L., Xia, Q., Shi, T. (2018). Stress-based topology optimization using bi-directional evolutionary structural optimization method. Computer Methods in Applied Mechanics and Engineering, 333, 356–370. doi: https://doi.org/10.1016/j.cma.2018.01.035
14. Abdi, M., Ashcroft, I., Wildman, R. (2018). Topology optimization of geometrically nonlinear structures using an evolutionary optimization method. Engineering Optimization, 50 (11), 1850–1870. doi: https://doi.org/10.1080/0305215x.2017.1418864
15. Hu, J., Yao, S., Gan, N., Xiong, Y., Chen, X. (2019). Fracture strength topology optimization of structural specific position using a bi-directional evolutionary structural optimization method. Engineering Optimization, 52 (4), 583–602. doi: https://doi.org/10.1080/0305215x.2019.1609466

16. Rahmatalla, S. F., Swan, C. C. (2004). A Q4/Q4 continuum structural topology optimization implementation. Structural and Multidisciplinary Optimization, 27 (1-2), 130–135. doi: https://doi.org/10.1007/s00158-003-0365-9
17. Talischi, C., Paulino, G. H., Pereira, A., Menezes, I. F. M. (2009). Polygonal finite elements for topology optimization: A unifying paradigm. International Journal for Numerical Methods in Engineering, 82 (6), 671–698. doi: https://doi.org/10.1002/nme.2763
18. Kunakote, T., Bureerat, S. (2011). Multi-objective topology optimization using evolutionary algorithms. Engineering Optimization, 43 (5), 541–557. doi: https://doi.org/10.1080/0305215x.2010.502935
19. Wallin, M., Ivarsson, N., Amir, O., Tortorelli, D. (2020). Consistent boundary conditions for PDE filter regularization in topology optimization. Structural and Multidisciplinary Optimization, 62 (3), 1299–1311. doi: https://doi.org/10.1007/s00158-020-02556-w
20. Kumar, P., Saxena, A., Sauer, R. A. (2016). Implementation of Self Contact in Path Generating Compliant Mechanisms. Microactuators and Micromechanisms, 251–261. doi: https://doi.org/10.1007/978-3-319-45387-3_22
21. Saxena, A. (2011). Topology design with negative masks using gradient search. Structural and Multidisciplinary Optimization, 44 (5), 629–649. doi: https://doi.org/10.1007/s00158-011-0649-4
22. Sukumar, N., Tabarraei, A. (2004). Conforming polygonal finite elements. International Journal for Numerical Methods in Engineering, 61 (12), 2045–2066. doi: https://doi.org/10.1002/nme.1141
23. Yoon, G. H., Ha, S. I. (2020). A New Development of a Shadow Density Filter for Manufacturing Constraint and Its Applications to Multiphysics Topology Optimization. Journal of Mechanical Design, 143 (6). doi: https://doi.org/10.1115/1.4048818
24. Yi, B., Yoon, G. H., Peng, X. (2020). A simple density filter for the topology optimization of coated structures. Engineering Optimization, 53 (12), 2088–2107. doi: https://doi.org/10.1080/0305215x.2020.1845326